

## High-resolution zero-kinetic-energy photoelectron spectroscopy of nitric oxide

M. Sander, L. A. Chewter, K. Müller-Dethlefs,\* and E. W. Schlag

*Institut für Physikalische and Theoretische Chemie, Technische Universität München,*

*Lichtenbergstrasse 4, D-8046 Garching, West Germany*

(Received 20 January 1987)

Rotationally selective photoionization dynamics for the transition  $(\text{NO}^+)X^1\Sigma^+(v^+=0, N^+) \leftarrow (\text{NO})A^2\Sigma^+(v=0, N_A, J_A=N_A+\frac{1}{2})$  is studied by high-resolution zero-kinetic-energy photoelectron spectroscopy (ZEKE-PES). Two-photon, two-color photoionization via the NO  $A$  state in a skimmed supersonic jet is employed in the experiments. The observed angular momentum transfer ion  $\leftarrow$  molecule is found to depend strongly on the initial quantum number  $N_A$ . The ionization potential is determined to be  $74719.0 \pm 0.5 \text{ cm}^{-1}$ .

### INTRODUCTION

Conventional photoelectron spectroscopy (PES), despite some effort, offers a typical energy resolution of around 10 meV ( $80 \text{ cm}^{-1}$ ) (Ref. 1) or at best around 5 meV ( $40 \text{ cm}^{-1}$ ).<sup>2</sup> For threshold PES (TPES) (Refs. 3 and 4) the resolution is only slightly better (3 meV). This lack of resolution prevents the observation of rotational structure in the ion except in a few cases, such as  $\text{H}_2^+$  (Ref. 5) and  $\text{D}_2^+$  (Ref. 4) or high- $J$  states of  $\text{NO}^+$ ,<sup>6</sup> where the rotational states are widely spaced. To this end our novel method of zero-kinetic-energy photoelectron spectroscopy (ZEKE-PES) has been developed. This method employs photoionization under field-free conditions (this avoids shifts and broadenings of thresholds) and application of a delayed pulsed extraction field. Detection of ZEKE electrons only and complete suppression of kinetic electrons is facilitated by seradancy and time-of-flight discrimination. Full details of the method, and results for NO and benzene have already been reported.<sup>7-9</sup>

In this paper we present results obtained from two-color laser ZEKE-PES of nitric oxide via different rovibronic levels of the vibrationless ( $v=0$ )  $A^2\Sigma^+$  state. The  $A$  state attends Hund's case  $b$  and the rotational levels are defined by the good quantum numbers  $J_A$  and  $N_A$  ( $J_A=N_A-S$ ). Here we use the ( $P_1$ )  $A \leftarrow X^2\Pi$  transition to populate the  $F_1$  rotational levels of the  $A^2\Sigma^+$  state with definite  $N_A$ ,  $J_A=N_A+\frac{1}{2}$  and parity  $(-1)^{N_A}$ .<sup>10</sup> The ground state of the ion  $X^1\Sigma^+$  is defined by rotational quantum numbers  $J^+=N^+$ .

### EXPERIMENT

The supersonic skimmed beam apparatus and ZEKE-PE analyzer have been described previously.<sup>7</sup> For the two-photon, two-color photoionization we employ two frequency doubled pulsed dye lasers of  $0.5 \text{ cm}^{-1}$  bandwidth in the uv (C450 and Sulforhodamine 101) pumped synchronously by the third and second harmonic of a Nd:YAG laser. Absolute calibration of the dye lasers to  $0.2 \text{ cm}^{-1}$  was carried out by comparison of the laser output and emission lines of a uranium lamp using a 1-m double-pass monochromator and a vidicon optical multichannel analyzer (OMA).

### RESULTS

Figures 1 to 4 show the ZEKE-PE spectra for ionization from  $J_A=\frac{1}{2}$  ( $N_A=0$ ),  $J_A=\frac{3}{2}$  ( $N_A=1$ ),  $J_A=\frac{5}{2}$  ( $N_A=2$ ), and  $J_A=\frac{7}{2}$  ( $N_A=3$ ), respectively. Each spectrum displays a number of discrete well-separated peaks corresponding to the rotational levels of the vibrationless  $X^1\Sigma^+$  ground state of the  $\text{NO}^+$  ion (the rotational quantum numbers  $N^+=J^+$  of the ion are indicated). In all spectra the photoionizing transitions for no change in rotation (i.e.,  $\Delta N=N^+-N_A=0$ ) are strongest. However, there are also important contributions for  $\Delta N \neq 0$  ionizing transitions. For  $N_A=0$  (Fig. 1) we observe transitions into  $N^+=2$ ,  $N^+=1$ , and  $N^+=3$ . The approximate intensities of these  $\Delta N \neq 0$  transitions are, compared to the  $N^+=0 \leftarrow N_A=0$  transition, 0.5 for  $\Delta N=2$ , 0.2 for  $\Delta N=1$ , and 0.1 for  $\Delta N=3$ . These  $\Delta N \neq 0$  transitions are not due to any peculiarities in the ionization cross section; we observe neither peaks nor dips in the ion yield spectrum (not shown) that could indicate autoionization effects or a changing coupling strength to dissociation continua.

For  $N_A=1$  (Fig. 2) we also find  $\Delta N \neq 0$  transitions, but the intensities relative to the  $N^+=1 \leftarrow N_A=1$  transition

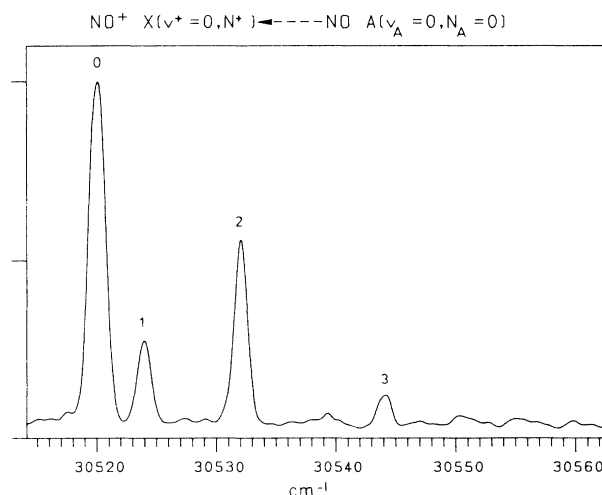
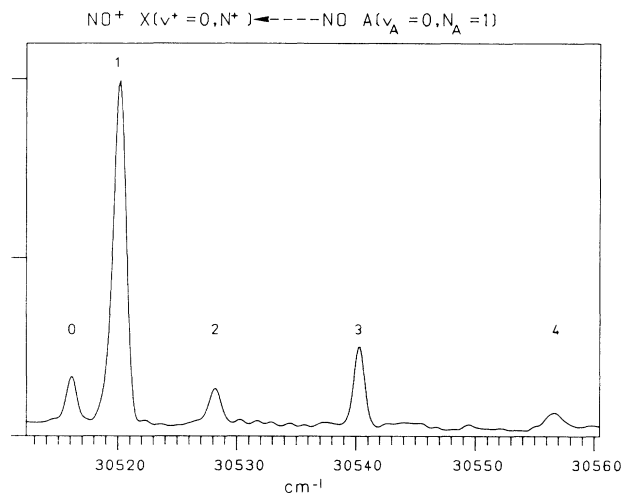
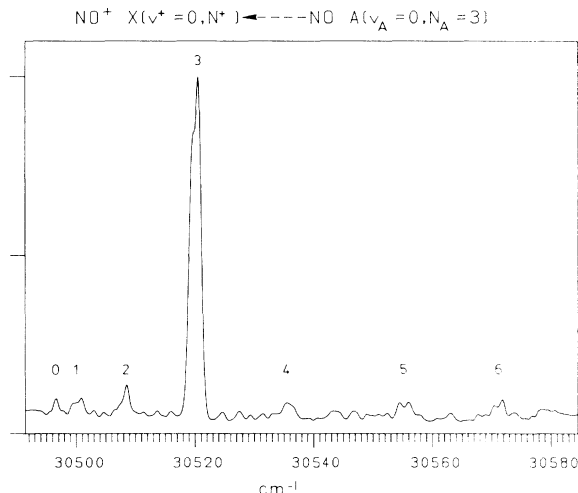
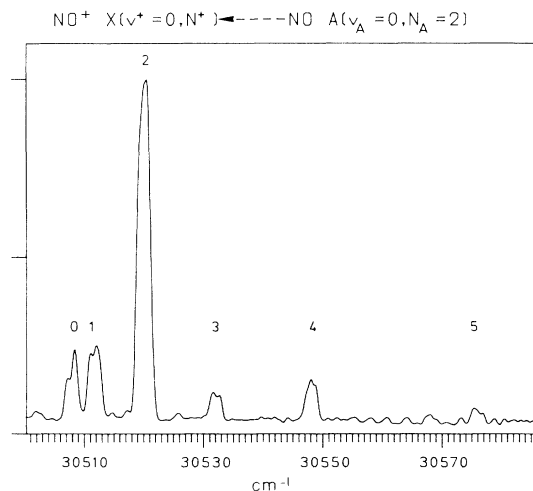


FIG. 1. ZEKE-PE spectrum for  $N_A=0$ ,  $J_A=\frac{1}{2}$  selected in the intermediate  $A^2\Sigma^+$  state.

FIG. 2. ZEKE-PE spectrum for  $N_A=1$ ,  $J_A=\frac{3}{2}$ .FIG. 4. ZEKE-PE spectrum for  $N_A=3$ ,  $J_A=\frac{7}{2}$ .

are smaller than for  $N_A=0$ . The intensities of the  $\Delta N \neq 0$  transitions (relative to  $N^+=2 \leftarrow N_A=2$ ) become even smaller for  $N_A=2$  (Fig. 3). For  $N_A=3$  (Fig. 4) the  $\Delta N \neq 0$  transitions are barely above the noise level and the spectrum is dominated by the  $N^+=3 \leftarrow N_A=3$  transition. Comparable intensities for  $\Delta N \neq 0$  transitions were obtained for high- $N_A$  values in PES.<sup>6</sup>

From the ZEKE-PE spectra and the  $A$  state term values<sup>11</sup> we determine a value for the ionization potential of  $74719.0 \pm 0.5 \text{ cm}^{-1}$ . The small discrepancy with our formerly reported value for the ionization potential [ $74717.2 \text{ cm}^{-1}$  (Ref. 9)] is due to our improved laser calibration. The extrapolation of identified Rydberg series leads to  $74719.3 \pm 2 \text{ cm}^{-1}$  (Ref. 12) and  $74721.5 \pm 0.5 \text{ cm}^{-1}$ .<sup>13</sup> Considering the rather different principles underlying ZEKE-PES and Rydberg extrapolations the agreement for the ionization potential obtained by both methods is remarkably good.

FIG. 3. ZEKE-PE spectrum for  $N_A=2$ ,  $J_A=\frac{5}{2}$ .

## DISCUSSION

The rather strong angular momentum transfer observed in the photoionization process and, in particular, the drastic decrease of the probabilities for  $\Delta N \neq 0$  transitions with increasing initial rotational quantum number  $N_A$  cannot be explained conclusively within this experimental paper. However, we want to discuss some applicable models. In the simplest model (a Rydberg electron moving in a purely Coulombic core potential)  $\Delta N \neq 0$  transitions cannot be explained. An electric dipole transition should change the orbital angular momentum of the electron by one, leaving the molecular rotation unchanged:  $\Delta l = \pm 1$ ,  $\Delta N = 0$ . Including the nonhydrogenic terms in the core potential for the  $\text{NO } A$  state results in a mixing of orbital angular momenta. For the  $A^2\Sigma^+$  ( $3s$  Rydberg) state recent *ab initio* calculations<sup>14</sup> quote 94%  $s$ , 0.3%  $p$ , and 5%  $d$  character for the  $6\sigma$  orbital. Since in Hund's case  $b$  the good quantum number  $N_A$  is the result of the coupling of the orbital angular momentum  $l$  of the electron and the mechanical rotation  $R$  of the molecule (neither alone is a good quantum number), for a given  $N_A$  such an  $l$  mixing corresponds to a mixing of mechanical rotational quantum numbers  $R_A$ . This leads to the selection rules:  $\Delta l = \pm 1$ ,  $\Delta(N^+ - R_A) = 0$  and implies finite probabilities for  $\Delta N = \pm 1, \pm 2$  transitions. Apart from the prediction of intensities, such models<sup>14</sup> still do not account for the strong decrease of  $\Delta N \neq 0$  contributions with increasing  $N_A$ . The reason for this failure<sup>14</sup> is the problem of generating accurate continuum wave functions, in particular, to account for the coupling of the orbital angular momentum of the outgoing photoelectron to the rotation via non-Coulombic terms in the core potential. Here we suggest a perturbation treatment for the non-Coulombic parts of the molecular core potential and we consider the terms in the continuum state Hamiltonian which scatter a particular partial wave of the outgoing electron into other partial wave channels, thereby changing the rotation of the core. These terms come from the interaction with the core's dipole and quadrupole moment as well as its polarizability,

TABLE I. Ionizing electric dipole transitions  $\text{NO}^+ \chi 1 \Sigma^+ (v^+ = 0, N^+) \leftarrow \text{NO} A^2 \Sigma^+ (v = 0, N_A = 0)$ .

Nonhydrogenic terms in the $A$ -state core potential	Initial state		
	$l = 0$ $R_A = 0$	$l = 1$ $R_A = 1$	$l = 2$ $R_A = 2$
Pure Coulombic core potential	Final state $l^+ = 1$ $N^+ = 0$	$l^+ = 0, 2$ $N^+ = 1$	$l^+ = 1, 3$ $N^+ = 2$
Dipole terms in the core potential	$l^+ = 0, 2$ $N^+ = 1$	$l^+ = 1, 3$ $N^+ = 0, 2$	$l^+ = 0, 2, 4$ $N^+ = 1, 3$
Quadrupole terms in the core potential and polarizability of the core	$l^+ = 1, 3$ $N^+ = 0, 2$	$l^+ = 0, 2, 4$ $N^+ = 1, 3$	$l^+ = 1, 3, 5$ $N^+ = 0, 2, (4)$

leading to the interaction operator  $V = H_{\text{quad}} + H_{\text{dipol}} + H_{\text{pol}}$ . Such long-range potentials were already successfully used to explain rotational autoionization effects of nonpenetrating  $f$  Rydberg states.<sup>15</sup> The effect of the various terms in the interaction Hamiltonian can be summarized as follows:

$$H_{\text{dipol}}: \Delta l = \pm 1, \quad \Delta(N^+ - R_A) = \pm 1,$$

$$H_{\text{quad}}, H_{\text{pol}}: \Delta l = \pm 2, \quad \Delta(N^+ - R_A) = \pm 2.$$

Hence, the effect of the interactions is  $l$  mixing in the continuum state. We can now determine the ionizing transitions with and without interaction in the continuum and for each of the angular momentum components in the  $6\sigma$  orbital of the  $A$  state. For  $N_A = 0$  these are summarized in Table I. For example, for the  $s$  component in the  $A$  state and the quadrupole interaction we obtain a rotational angular momentum transfer of up to  $\Delta N = N^+ - N_A = 2$ . With the  $p$  component in the  $A$  state and the dipole interaction we can explain the observed  $\Delta N = 3$  transition (Fig. 1). This is similar to the interpretation of Rydberg-Rydberg transitions from the  $A$  state to  $s$ ,  $p$ ,  $d$ , and  $f$  Rydberg series.<sup>16</sup>

A change of  $N_A$  from 0 to 3 corresponds to an energy increase of only  $24 \text{ cm}^{-1}$  in the  $A$  state. On such an energy scale considerable changes of  $l$  coupling to the axis of  $l$  mixing in the  $A$  state cannot be expected. We therefore attribute the decrease of the  $\Delta N \neq 0$  transitions with increasing  $N_A$  to the energy dependence of the interactions in the continuum state. If one ignores interference effects, a simple picture may be drawn: First a  $\Delta(N^+ - R_A) = 0$  Rydberg or continuum state is excited (rate constant  $p_1$ ); the interaction operator  $V$ , however, mixes in continuum states with  $\Delta(N^+ - R_A) \neq 0$  (contribution  $p_2$ ). The rate constant  $p$  for a  $\Delta(N^+ - R_A) \neq 0$  transition is then  $p = p_1 \cdot p_2$ . The expressions for  $p_1$  and  $p_2$  may be taken from Fermi's "golden rule" and first-order perturbation theory, respectively.

$$p_1 \propto |\langle R_A, l \pm 1 | \mu | R_A, l \rangle|^2 \rho(E_{N^+} - E_R),$$

$$p_2 \propto \frac{|\langle N^+, l^+ | V | R_A, l \pm 1 \rangle|^2}{[B^+ N^+ (N^+ + 1) - B^+ R_A (R_A + 1)]^2}.$$

$B^+$  is the rotational constant of the ion,  $\mu$  is the electric dipole operator, and  $\rho(E_{N^+} - E_R)$  corresponds to the den-

sity of  $\Delta(N^+ - R_A) = 0$  Rydberg or continuum states. Since we detect only ZEKE photoelectrons these Rydberg or continuum states have to be isoenergetic to the  $\Delta(N^+ - R_A) \neq 0$  ionic levels. For  $\Delta(N^+ - R_A) > 0$  the density of states is constant, for  $\Delta(N^+ - R_A) < 0$ , however, it depends on the energy difference to the  $N^+ = R_A$  threshold and decreases as the energy difference increases. From quantum defect theory it is known that the matrix elements should only weakly depend on energy near threshold (here we consider energy differences which are  $\approx 10^{-4}$  of the ionization energy). However, the strong energy dependence is brought in by the denominator in  $p_2$ . As the spacing between adjacent rotational levels increases linearly with the rotational quantum number this leads to a quadratic increase of the denominator in the expression for  $p_2$ .

The importance of the density of states becomes apparent when comparing the  $\Delta(N^+ - R_A) > 0$  and  $\Delta(N^+ - R_A) < 0$  transitions, for example, the relative intensities of the  $N^+ = 3 \leftarrow N_A = 0$  (Fig. 1) and the  $N^+ = 0 \leftarrow N_A = 3$  (Fig. 4) transitions. For  $\Delta(N^+ - R_A) < 0$  contributions the relative intensity is lower due to the density of available Rydberg states: around  $N^+ = 0$  ( $24 \text{ cm}^{-1}$  below the  $\Delta N = 0$  threshold for the  $N^+ = 3 \leftarrow N_A = 3$  transition) the spacing between Rydberg states with subsequent principal quantum numbers  $n$  is of the order of  $1 \text{ cm}^{-1}$ . If, therefore, Rydberg and ionic levels do not coincide very well energetically, the probability for the detection of a ZEKE photoelectron can go to zero, an effect that cannot be compensated for by the increase of the oscillator strength for lower principal quantum numbers  $n$ . Both effects, the energy dependence of the denominator and of the density can, at least qualitatively, account for the drastic decrease of angular momentum transfer observed for higher  $N_A$  values.

## CONCLUSIONS

ZEKE-PES has proved to be an important tool for the investigation of the dynamics in molecular photoionization processes. Transitions involving rather high angular momentum transfer are observed near threshold. To understand these changes of the rotational state and, in particular, their strong dependence on the initial molecular

rotation, it is suggested here that one must consider the coupling of the electron to the nonhydrogenic terms in the molecular core potential. This is done not only for the bound molecular state but also for the continuum state, since the outgoing photoelectron can still interact with the long-range potential of the core.

---

\*Author to whom correspondence should be addressed.

- <sup>1</sup>D. W. Turner, *Molecular Photoelectron Spectroscopy* (Wiley, London, 1970).
- <sup>2</sup>S. R. Long, J. T. Meek, and J. P. Reilly, *J. Chem. Phys.* **79**, 3206 (1983).
- <sup>3</sup>T. Baer, W. B. Peatman, and E. W. Schlag, *Chem. Phys. Lett.* **4**, 243 (1969).
- <sup>4</sup>W. Peatman, F. P. Wolf, and R. Unwin, *Chem. Phys. Lett.* **95**, 453 (1983).
- <sup>5</sup>J. E. Pollard, D. J. Trevor, J. E. Recett, Y. T. Lee, and D. A. Shirley, *J. Chem. Phys.* **77**, 34 (1982); L. Asbrink, *Chem. Phys. Lett.* **7**, 549 (1970).
- <sup>6</sup>K. S. Viswanathan, E. Sekreta, E. R. Davidson, and J. P. Reilly, *J. Phys. Chem.* **90**, 5078 (1986).
- <sup>7</sup>K. Müller-Dethlefs, M. Sander, and E. W. Schlag, *Z. Naturforsch. Teil A* **39**, 1089 (1984).
- <sup>8</sup>L. A. Chewter, M. Sander, K. Müller-Dethlefs, and E. W. Schlag, *J. Chem. Phys.* **86**, 4737 (1987).
- <sup>9</sup>K. Müller-Dethlefs, M. Sander, and E. W. Schlag, *Chem. Phys. Lett.* **112**, 291 (1984).
- <sup>10</sup>G. Herzberg, *Spectra of Diatomic Molecules* (Van Nostrand, New York, 1950).
- <sup>11</sup>C. Amiot and J. Verges, *Phys. Scr.* **25**, 302 (1982).
- <sup>12</sup>M. Seaver, W. Chupka, S. D. Colson, and D. Gauyacq, *J. Phys. Chem.* **87**, 2226 (1983).
- <sup>13</sup>E. Miescher, *Can. J. Phys.* **54**, 2074 (1976); Chr. Jungen and E. Miescher, *ibid.* **47**, 1769 (1969).
- <sup>14</sup>S. N. Dixit, D. L. Lynch, V. McKoy, and W. M. Huo, *Phys. Rev. A* **32**, 1267 (1985).
- <sup>15</sup>E. E. Eyler and F. M. Pipkin, *Phys. Rev. A* **27**, 2462 (1983); E. E. Eyler, *ibid.* **34**, 2881 (1986).
- <sup>16</sup>W. Y. Cheung, W. A. Chupka, S. D. Colson, D. Gauyacq, P. Avouris, and J. J. Wynne, *J. Chem. Phys.* **78**, 3625 (1983).